Parametric resonance enhancement in neutron interferometry and application for the search for non-Newtonian gravity

Vladimir Gudkov, Hirohiko. M. Shimizu, and Geoffrey L. Greene

Parametric Resonance Enhancement in Neutron Interferometry and Application for the Search for Non-Newtonian Gravity

Vladimir Gudkov

Department of Physics and Astronomy, University of South Carolina,

Columbia, SC 29208

Hirohiko. M. Shimizu

High Energy Accelerator Research Organization (KEK),

1-1 Oho, Tsukuba, Ibaraki 305-0801, Japan

Geoffrey L. Greene

Department of Physics, University of Tennessee, Knoxville, TN, 37996, and

Physics Division, Oak Ridge National Laboratory, Oak Ridge, TN, 37831

Abstract

The parametric resonance enhancement of the phase of neutrons due to non-Newtonian anomalous gravitation is considered. The existence of such resonances is confirmed by numerical calculations. A possible experimental scheme for the observation of this effect is discussed based on an existing neutron interferometer design.

Introduction

Precision experimental tests of Newtonian gravity utilize a wide range of techniques to search for the existence of possible "anomalous" couplings between massive objects. (See Adelberger, *et al.*[1] for a comprehensive review). Recently, these searches have been stimulated by theoretical models which consider the possible existence of "non-$1/r^2$" gravitational forces at distances on the sub-millimeter scale. These models (see, for example [2][3][4][5] and references therein) propose mechanisms of gravitational unification based on the existence of extra dimensional space with compactified extra dimensions and/or with large extra dimensional bulk space. Such forces may be viewed as arising from gravity being allowed to propagate in a whole space (bulk) with extra dimensions while particles and interactions of the Standard Models are confined inside of our three dimensional space (3-brane). Some approaches to resolve the cosmological constant paradox (hierarchy problem) also lead to modified gravity at short distances (see for example [6][7]). It has also been noted[8][9] that the scale of the "dark energy" density ($\sim 10^{-3}$ $eV)^4$ is close to the characteristic energy scale for very low energy neutrons and suggests the possible sensitivity of neutrons for tests of gravity at corresponding length scales (< 0.1 mm). A more exotic source of a possible modification of Newton's gravity at short distances – "ungravity" [10] results from a nontrivial scale invariant sector of an effective field theory which cannot be described in terms of particles[11]. For these, as well as other, perhaps even aesthetic reasons, it is desirable to test predictions of modified gravitational forces over the widest possible range. As a neutral, heavy, relatively non-polarizable and almost stable particle, the neutron provides an attractive probe for anomalous gravitational forces with ranges from nuclear sizes up

to the macroscopic scale. As we shall discuss, the use of neutrons of extremely low energy can lead to enhanced sensitivities to possible interactions with a comparable (very small) characteristic energy scales. Indeed, the scattering of cold and thermal neutrons as well as measurements with ultra cold neutron experiments have been used to set some of the best constraints on anomalous gravity at short range [1] [12] [13] [14] [15].

As is conventional in this field, we assume that a hypothetical, short range non-Newtonian interaction is given by [1] (see also [16])

$$V(r) = -\frac{GMm}{r}(1 + \alpha_G e^{-r/\lambda}), \tag{1}$$

where G is the gravitational constant, m and M are the interacting masses, α_G is a dimensionless parameter reflecting the strength of the anomalous interaction and λ is its effective range.

In a recent paper [17] a method to search for exotic gravitational interactions using neutron interferometry was proposed. In that work, it was observed that, under certain conditions, it might be possible to satisfy certain parametric resonance conditions that would provide a greatly enhanced sensitivity to anomalous forces. In this work we consider the case of very low energy neutrons (so called very cold and ultra cold neutrons with E<< 1 meV) to explore the conditions under which such resonant enhancement could be used to substantially improve constraints on "exotic" interactions.

Parametric Resonance

We consider the "two slab" interferometer setup suggested in [17]. The anomalous interaction of Eq. (1) leads to a potential for a neutron propagating over a plate of matter of uniform density ρ, as a function of x, the distance from the surface:

$$V_{eff} = 2\pi G \alpha_G m_n \rho \lambda^2 e^{-x/\lambda} \qquad \text{outside the material;}$$

$$V_{eff} = 2\pi G \alpha_G m_n \rho \lambda^2 (2 - e^{-x/\lambda}) \qquad \text{inside the material.}$$

To calculate the phase shift due to this interaction we use the exact solution of Schrödinger's equation for neutron propagation through two parallel plates of similar material separated by distance L under the assumption that the size of the plates are much larger than both the distance L and the range of the short gravitational interaction λ (for details see reference [17]). It was noted [17] that the solution of this problem suggests the possible parametric resonance enhancement of the phase shift due to anomalous interactions during neutron propagation through the slabs. This suggestion is confirmed by an exact solution of Schrödinger's equation. Unfortunately, while an analytic solution for this problem has been obtained, the expression for the neutron phase is rather complicated and is far too long to be presented here. As a consequence, while this solution implicitly includes parametric resonances, it does not do so in a transparent manner. For a simple illustration of the existence of such parametric resonances, we will therefore first show the general conditions for the existence of the resonances using a "toy" theoretical model and then discuss why very low neutron energies are crucial. Finally we will confirm the suggestions of the "toy" model by numerical solution of the exact Schrödinger equation.

Schrödinger's equation for neutron propagation in between the slabs can be written as

$$d^2\psi(x)/dx^2 + k^2(x)\psi(x) = 0 , \tag{2}$$

where

$$k^2(x) = k_0^2(1 + \eta\cosh(x/\lambda)) ,$$

$$\eta = 2a^2\exp(-L/2\lambda)/k_0^2 ,$$

$$a^2 = 4\pi G\alpha_G m_n^2\rho\lambda^2/\hbar^2 ,$$

and k_0 is the neutron wave number in vacuum. This is Mathieu's modified differential

equation and its general solution is represented in terms of Mathieu functions (instead

of exponential functions in the case of the square-well potential). That the neutron

transmission coefficient results from a solution of a Mathieu - type equation (often

used to describe parametric resonances) suggests the possibility of observing an

enhancement in neutron propagation provided the proper resonance conditions are

satisfied. It should be noted that similar parametric resonances are a common

phenomena in optics: see, for example, refs. [18] [19] for parametric resonances in optical

resonators and refs. [20] [21] for resonances for light propagation through paraxial optical

systems. A similar phenomenon has been discussed for the coherent propagation of

neutrinos through materials with a variation of density profile (see, for example

papers [22] and references therein). The parametric resonance (PR) enhancement of

neutrino oscillations has been calculated for a variation of density of material over

only "one and a half" periods of density modulation [22].   These calculations

demonstrate that PR can exist in transmission processes without a requirement of

"pure" periodic structure of density profile variations.

A quantum PR in a process of one dimensional particle transmission is not a new

phenomenon. To our knowledge, L. P. Pitaevsky (see [23] and references therein) first

pointed out that the solution of the one-dimensional Schrödinger equation for the

harmonic oscillator exactly coincides with the solution of the one-dimensional

potential barrier propagation problem (provided that the transmitted particle

momentum $k(x)$, as a function of distance, is replaced by the frequency of the

harmonic oscillator as a function of time in the Schrödinger equation). The

correspondence of the solutions for these two problems (harmonic oscillator and

transmission) was studied [23] for the case of the exactly solvable Eckart's potential

[24] which analytically exhibits the existence of quantum parametric resonance

(quantum parametric amplifier [23]). Using a similar approach, we analyze the

conditions for the existence of PR in the case of neutron transmission in the "two

slab" scenario in the presence of short range gravity. Unfortunately, even the simplest

case for the calculation of the transmission amplitude involves at least three coupled

Schrödinger equations which make analytic analysis practically impossible.

Therefore, to be able to qualitatively understand the main features of the solution and

to obtain a general feature of PR in the transmission amplitude we consider a very

simple "toy" model (see Appendix A) which indicates the possibility of the existence

of PR for long neutron wavelengths.

We emphasize that we are dealing with a resonance enhancement of the *phase* of the

transmission coefficient for neutron propagation. This particular subject has not been

explicitly considered in the literature related to *transmission* in one dimensional

barrier problems. Reconsideration of a number of well-known solutions of

Schrödinger's equation for the transmission problem does, however, indicate the

possibility of resonance phase enhancement in the one-dimensional

scattering/transmission process. For example, it has been shown [25] that the

transmission amplitude for an exponentially decreasing potential has an infinite

number of singularities in the complex momentum plane (for a general description of

the phase in one dimensional scattering see refs. [26] [27]). The position of the singularity

nearest to the real axis is defined only by the slope of the potential and not by its

value. For a pure exponential potential, the nearest singularity lies on the imaginary

axis. It was pointed out [25] that, for the case of two overlapping potentials,

corresponding to the situation considered in this paper, the transmission amplitude has

a second order pole at the same position defined only by the slope, $k = -2i / \lambda$. This

implies that when the neutron wavelength, λ_n is comparable to the scale of the

anomalous gravitational interaction, λ, the phase of the transmission amplitude is

most sensitive to this interaction. It is important that the minimal distance of the

singularities from the real axis is not zero and that the poles are allowed to move off

the imaginary axis for a non-pure exponential potential.

It is notoriously difficult to prove the existence of PR for any system other than the

simplest ones since PR is related to unstable solutions which cannot be treated by

conventional methods of solution or by perturbation theory. We do not have a proof

for existence of PR for the phase of the transmission coefficient. Instead, as a

plausibility argument, we explore a number of approaches to show the existence of

unstable solutions of the phase of transmission coefficient (see Appendix B). The

phase is unstable if it has a branch of exponentially growing (unstable) solution. One

can see such solutions with a typical behavior

$$\varphi(x) \sim a\lambda_n \exp(x / \lambda) \tag{3}$$

in perturbation theory approach, for asymptotic solutions, and for available exact

solutions of the problems with solvable exponentially dependent potentials.

The above proportionality to the neutron wavelength explains why PR could be seen

only in the case of very cold neutrons.   It should be noted that unstable solutions

were also observed for inverse power potentials, such as would result from anomalous gravitational interactions (see, for example [1] and references therein). Thus the existcnce of PR (unstable solutions) for the phase of transmission through singular (exponential or inverse power) potentials in neutron interferometry is highly plausible.

To illustrate the sensitivity of the phase of the transmission amplitude to the slope of the potential, we consider a "toy" model for neutron transmission barrier which consists of two potentials: the first is a localized strong potential due to the nuclear interaction between the neutron and material and the second is a weak exponentially decreasing potential. The amplitude T for neutron transmission through the sum of these potentials is proportional to the product of the two transmission amplitudes for each potential separately, see [28],

$$T \sim t_s t_w. \tag{4}$$

If one potential is very weak compared to the other one, its transmission coefficient is, for all practical purposes, governed by the properties of the strong potential, $|T|^2 \sim |t_s|^2$. The phase of T, however, is sensitive to the total phase of both t_s and t_w:

$$Arg(T) = Arg(t_s) + Arg(t_w) + ... \tag{5}$$

For the first order pole ($t_w \sim 1/(k + 2i/\lambda)$), the weak amplitude phase could be as much as:

$$Arg(t_w) \sim \tan^{-1}(\pi\lambda_n/\lambda). \tag{6}$$

For the second order pole ($t_w \sim 1/(k + 2i/\lambda)^2$),

$$Arg(t_w) \sim \tan^{-1}\left(\frac{2(\pi\lambda_n/\lambda)}{(\pi\lambda_n/\lambda)^2 - 1} \right). \tag{7}$$

This implies that, if the neutron wavelength is comparable to λ, the phase of neutron transmission coefficient will be very sensitive to small exponentially decreasing

potentials. This rather surprising observation is confirmed by cases with exact analytical solutions for transmission through potential barriers with exponentially dependent potentials (see, for example, Eckart's potential [24], and a number of other solved problems [29] [30]). For these cases, the transmission amplitudes are meromorphic functions with the positions of their poles dependent on the value of the exponential slopes, but not on the value of the potentials themselves (see also [27]).

Consideration of such toy-models suggests that an enhanced sensitivity to the gravitational potential for the phase of the transmission coefficient will occur when the neutron wavelength is comparable to the scale of the anomalous gravitational interaction and to the spacing between the two slabs in the interferometric experiment. This condition is consistent with the requirements for the existence of parametric resonance and shows the particular sensitivity of ultra-cold neutrons to such hypothetical weak interactions. We reiterate that the formulae discussed above were obtained using a number of simplifications to allow compact analytical expressions. They can only be used to provide a qualitative understanding of the process. Realistic estimates of the magnitude of possible manifestations of the PR must follow from exact numerical calculations [17] in the low energy range where observable effects are anticipated. For example, a null result from the "two slabs" experimental setup [17] with the neutron wavelength $\lambda_n = 30$ nm, a fixed slab separation $L = \lambda$, and a phase sensitivity of 10^{-3} radian, generates a very narrow resonance in the exclusion plot, see Fig.1.
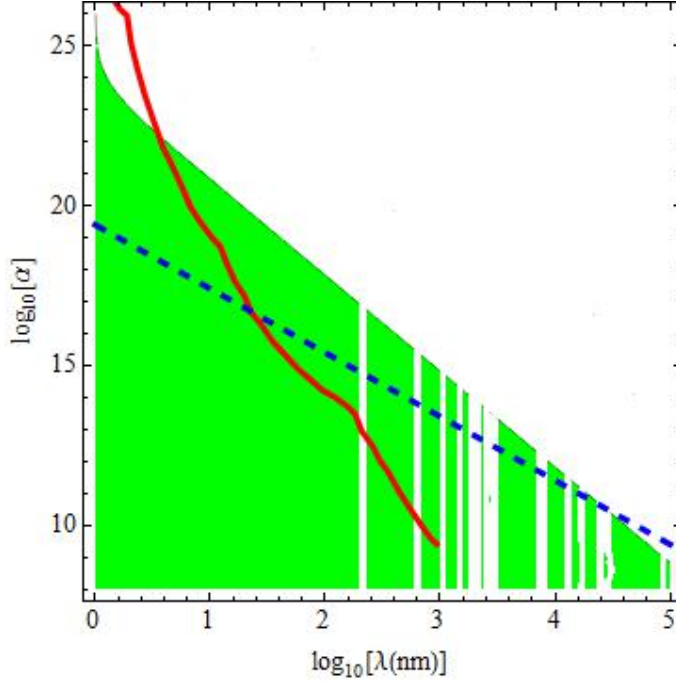
Fig. 1: (Color online) Exclusion plot for $\lambda_n = 30$ nm the separation $L = \lambda$ assuming an experimental sensitivity to the phase at the level 10^{-3} radian. The solid line shows current exclusion [1] and the dashed line a possible exclusion from Bragg-scattering experiment [21], the white area above the shaded regions can be excluded by the proposed experiment.

As a demonstration of the sensitivity of the method, we calculated excluded regions (Fig. 2) for the discussed setup for $\lambda_n = 30$ nm with the same experimental sensitivity to the phase at the level 10^{-3} radian by scanning the distance between the slabs from $L = 0.5 \lambda$ to $L = 5 \lambda$ with a step 0.5λ.
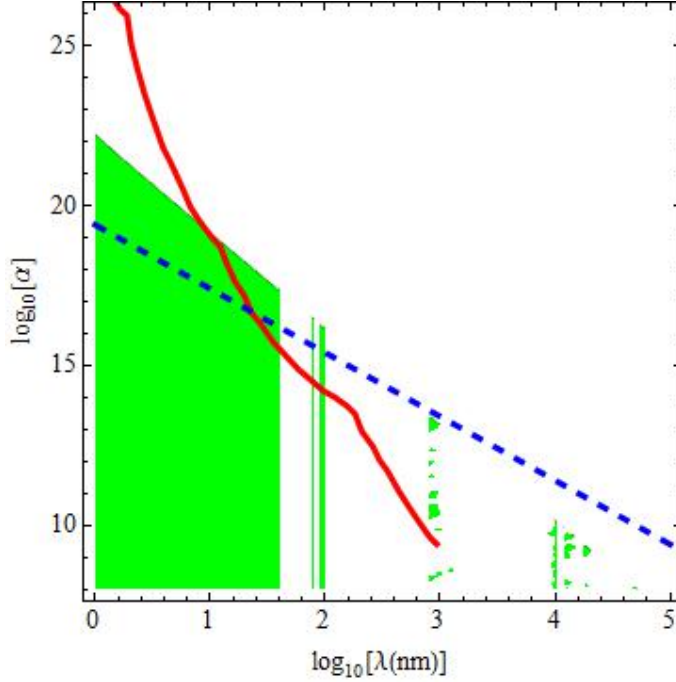
Fig. 2: (Color online) Exclusion plot for $\lambda_n = 30$ nm and the experimental sensitivity

to the phase at the level 10^{-3} radian by scanning the distance between the slabs from

$L = 0.5\,\lambda$ to $L = 5\,\lambda$ with a step $0.5\,\lambda$. . The solid line shows current exclusion [1] and

the dashed line a possible exclusion from Bragg-scattering experiment [17], the white

area above the shaded regions can be excluded by the proposed experiment.

It should be noted that the exclusion region (the white area above the shaded regions)

in Figs. 1 and 2 can go below the bottom horizontal axis which is a typical feature for

an ideal parametric resonance. In a real situation the depth of the excluded regions

will be constrained by a number of factors such as energy resolution, roughness of the

surface etc. Simple simulations show that it is unlikely to have a depth for the

exclusion area lower than $\alpha = 10^5$. However, the estimate of the possible depth is

beyond of the scope of this paper because it essentially depends on the specific

features of an apparatus.

For Figs. 1 and 2 we assumed monochromatic neutrons. To show how the parametric resonance is sensitive to the non-monochromaticity of the beam, we calculated the phase of the transmission amplitude for a small value of $\alpha=10^{5.5}$ (where PR became extremely narrow), with $L = 2\lambda$ as a function of the range of "gravitational" interaction for monochromatic neutrons of $\lambda_n = 30$ nm (Fig. 3a), and for a 1% energy spread assuming a flat distribution (Fig.3b).
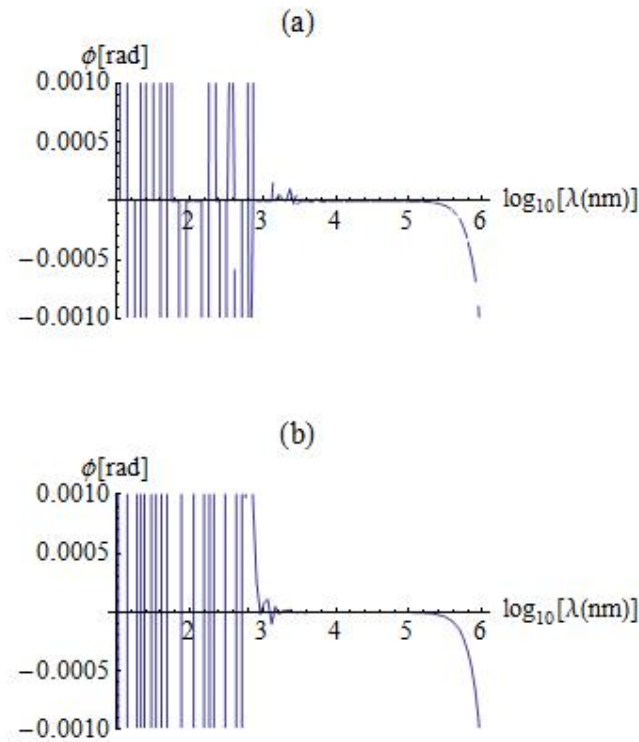
(a)

(b)

Fig. 3: (Color online) "Gravitational" phase for $\alpha=10^{5.5}$ and $L = 2\lambda$ as a function of the range of "gravitational" interaction for (a) monochromatic neutrons with $\lambda_n = 30$ nm, and (b) for 1% of energy resolution for neutrons.

One can see that the number of parametric resonances as well as their positions are changed. It is particularly notable that the phenomenon of parametric resonances exists even for a non-monochromatic beam. A typical behavior of the "gravitational

phase" as a function of separation, L, for two values of λ is shown in Fig. 4. Fig. 5

shows the "gravitational phase" as a function of α_G for a fixed L and λ.

$\lambda=100\text{nm}$

$\phi[\text{rad}]$

6
5
4
3
2
1

610   620   630   640   650   660 $L(\text{nm})$

$\lambda=50\text{nm}$

$\phi[\text{rad}]$

6
5
4
3
2
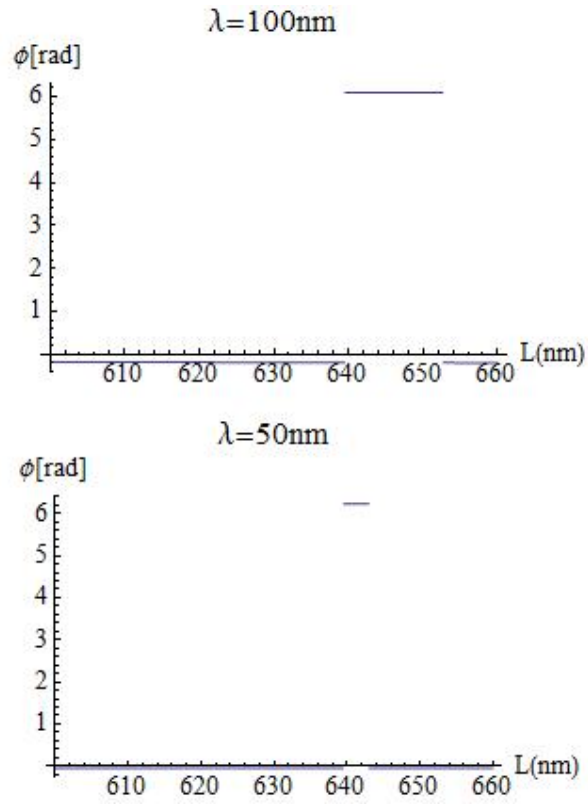1

610   620   630   640   650   660 $L(\text{nm})$

Fig. 4: (Color online) "Gravitational phase" as a function of separation, L, for two

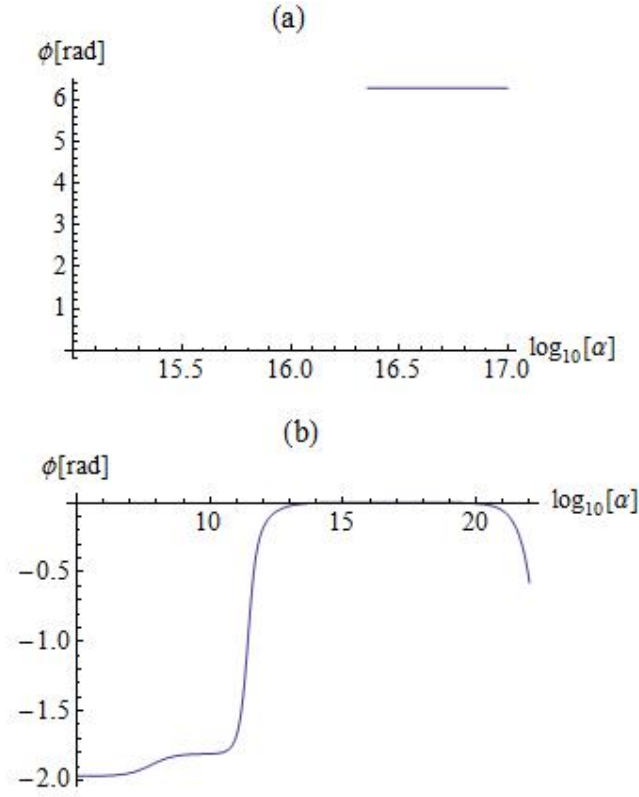values of $\lambda=100\text{nm}$ and $\lambda=50\text{nm}$. ($\lambda_n = 30$ nm and $\alpha=10^{19}$).

Fig. 5: (Color online) "Gravitational phase" as a function of α_G (a) L=639.55nm and λ=100nm, and (b) L=123nm and λ=12.3nm ($\lambda_n = 30$ nm).

It should be noted that when the neutron energy is very low, there are a number of "regular" Fabri-Perot type of resonances which exist for the given experimental setup without short-range "gravity." This "Fabri-Perot" multiple reflection of the neutron beam in between the slabs is modulated by the short-range interaction resulting in the parametric resonance, provided the resonance conditions are satisfied.

Such resonances can mimic the PR enhanced gravitational effects. Fortunately, these two types of resonances have essentially different dependences on the parameters (geometry, neutron wavelength, and $\alpha\lambda^2$) and can therefore be separated if the experiment is done with two or more different neutron wavelengths.

These numerical results confirm the simplified "toy" analysis and provide the first detailed exploration of phase parametric resonance in neutron interferometry. We note that although the effects suggested by the above analysis are very small, they may be accessible by using a new type of neutron interferometer. In the next section we discuss a possible experimental approach which looks promising for observing parametric resonance enhancement of neutron transmission phase.

Experimental Realization

As noted above, the use of very low energy neutrons (with correspondingly long wavelengths) can provide an enhanced sensitivity to possible phase changes resulting from parametric resonances induced by anomalous gravity. However, in the most commonly used neutron interferometers, which are based on neutron diffraction by silicon single crystals [31], the accessible neutron wavelengths are limited to being shorter than twice the silicon lattice constant. In practice, this implies the use of thermal neutrons with wavelengths less than a few tenths of a nanometer. Interferometry that is not based upon perfect crystal diffraction is not so limited in and it is possible to increase the wavelength range of neutron interferometry through the use of mirror optics and/or artificial multilayers rather than perfect crystal lattices. The prospect of extending neutron interferometry to cold and very-cold wavelength regions has been demonstrated by Kitaguchi et al. [32], who used optical elements

consisting of artificial multilayer mirrors. Their interferometer consisted of two pairs of mirrors deposited on precision air-gap etalons.

The Kitaguchi et al. multilayer interferometer was a Jamin-type neutron spin interferometer that used $\lambda_n = 0.88$ nm neutrons as schematically shown in Fig. 6 and Fig. 7. Spin polarized neutrons were directed to the interferometer through a $\pi/2$-flipper to define the phase relation between two magnetic substates. The relative phases of these states evolved during propagating in the external magnetic field applied parallel to the y-axis (equivalent to the spin rotation on zx-plane). The neutrons then hit a magnetic mirror and a non-magnetic mirror deposited on the inner surfaces of an air-gap etalon. The magnetic mirror reflects only one magnetic substate while the non-magnetic mirror reflects both. The spin direction was then reversed by a π-flipper before reflected on the second etalon. The spin polarization after another $\pi/2$-flipper depends upon the integrated phase difference accumulated between the two magnetic substates.

In the following we consider a possible experimental arrangement which would be sensitive to a parametric resonance enhanced phase due to anomalous gravity. We assume a Kitaguchi type interferometer, with minimal modification from that described in the reference [32], installed on the VCN port of the PF-2 beam line at the Institut Laue Langevin Research Reactor [33] [34]. In this paper, we do not discuss the VCN interferometer with grating plates reported in the reference [35], since it is not straightforward to spatially separate neutron paths with the grating-plate interferometer.

The phase accuracy for an interferometer can be approximately given by,

$$\Delta\phi = \frac{1}{K\sqrt{N}},\qquad\qquad (11)$$

where K is the visibility of the interferometer and N is the number of neutrons contributing to the measurement. We use the experimental result of $K=0.6$ in Ref. [32] for the visibility. N can be estimated as

$$N = \frac{\Phi}{\Delta v_x \Delta v_y}\Delta v_z V_{XY} T t.\qquad\qquad (12)$$

For the beamline under consideration, $\Phi = 10^4$ cm^{-2} s^{-1} (m/s)$^{-1}$ is the VCN flux at a neutron wavelength of $\lambda_n = 30$ nm ($v_z = 13$ m s^{-1})[33,34]. Δv_x and Δv_y are the beam divergences along x and y direction, respectively. We assume that the beam divergence is limited by natural nickel guide, which corresponds to $\Delta v_x = \Delta v_y = 14$ m s^{-1}. Δv_z is the width of the parametric resonance in terms of the neutron velocity, and V_{XY} is the acceptance of the interferometer. T is the overall transmission of the interferometer and t is the measurement time. We assume that $\Delta\lambda_n / \lambda_n \approx 0.01$ following the assumption in the numerical calculations shown in Fig. 3b which implies $\Delta v_z = v_z \Delta\lambda_n / \lambda_n = 0.13$ m s^{-1}.

We assume a sample as in Ref. [17], that consists of two dense material slabs that are separated by a well-controlled thin gap L. The neutron phase change due to the exponential decaying potential resulting from the hypothesized anomalous gravitational interaction can be measured by adjusting the position of the material plate so that one beam path transmits through the gap region and the other through the

"gap-less" region. We assume that we can obtain a surface roughness of the order of 0.1 nm using precision machining and polishing techniques[42].

Two beam paths of the principal ray are $P_0P_1P_2P_3P_4P_5P_6P_{11}P_{12}P_{13}$ and $P_0P_1P_2P_7P_8P_9P_{10}P_{11}P_{12}P_{13}$ as shown in Fig.7. They must be spatially separated between the two etalon sets. The separation defines the acceptance V_{XY} of the interferometer. For simplicity, we assume that the etalons have a square shape. We assume that the dimension of etalon substrates is $w_E \times w_E \times t_E$ and multilayer mirrors are deposited on the central square of $w_M \times w_M$ as shown in the right top inset of Fig. 6. We conserve the area of etalons and mirrors by taking the values of $w_E = 4.2 \times \sqrt{\pi}/2$ cm $= 3.7$ cm and $w_M = 2.0 \times \sqrt{\pi}/2$ cm $= 1.8$ cm. We also assume the thickness of the etalon substrate is $t_E = 1$ cm. In the reference [32], the air-gap was $g_E = 9.75 \times 10^{-4}$ cm and the distance between two etalon sets was $D = 34$ cm. The effective lattice constant of the multilayer mirror was $d = 24$ nm, which corresponded to $\sin\theta = h/(2mv_z d) = 0.63$, where θ is the grazing angle to the etalon surface, h is the Planck's constant and m is the neutron mass. In this estimate, the neutron refraction and the energy change on the material surface must be taken into account since the neutron kinetic energy $E \sim 9.1 \times 10^{-7}$ eV is close to the Fermi potential of the etalon substrate $U \sim 1.0 \times 10^{-7}$ eV (SiO$_2$). The grazing angle of the etalon substrate Θ is given as $\sin\Theta = 0.56$ through the relation

$$\sin^2\theta = (1 - \frac{U}{E})\sin^2\Theta + \frac{U}{E} \ .$$

We take the effective lattice constants of non-magnetic and magnetic mirrors as $d = 24$ nm and $d' = 28$ nm, respectively.

The spatial separation of individual beam paths between two etalon sets is $w_x = 2g_E \cos\theta$. We assume the spatial acceptance along y-axis is filled ($w_y = w_M$). Consequently, the hatched region in the left inset of Fig. 6 is the allowed region and the acceptance is given as

$$V_{XY} = \left(w_x \frac{w_x v_z}{D} \right) \times \left(w_M \frac{w_M v_z}{D} \right),$$

under the condition that the etalon size is small compared with the distance between two etalons.

The overall transmittance for two beam paths is given as

$$T = \frac{1}{2}(1-R_1)^2(1-R_2)^2 \left(\exp(-n\sigma_{abs}t_P) \right) \left(\exp\left(-n\sigma_{abs} \frac{t_E}{\sin\Theta} \right) \right)^4,$$

where the factor of 1/2 is the transmittance of the ideal polarizer, $R_1 = 7.3 \times 10^{-3}$ and $R_2 = 1.7 \times 10^{-2}$ are the reflectivities on the etalon surface for neutrons entering into the and exiting from the substrate, t_P the thickness of the material plate, n the number density and σ_{abs} the absorption cross section of the SiO_2 molecule. Here it is assumed that the coherent scattering is sufficiently suppressed and the small angle neutron scattering in etalon substrates is negligibly small (reasonable for a perfect crystal SiO_2). We assumed that the reflectivity of the non-magnetic mirror is 100% and the reflectivity of the magnetic mirror is 0% and 100% for each spin state. The absorption cross section is estimated as $\sigma_{abs} = 29$ b extrapolating the thermal absorption cross section assuming the absorption cross section is inversely proportional to neutron velocity. We take the thickness of the material plate as $t_P = 1$ mm. Consequently the transmittance of two beam paths of principal rays is estimated to be $T = 5.0 \times 10^{-3}$.

For this arrangement a phase accuracy of $\Delta\phi = 10^{-3}$ requires a measurement time of $t = 4 \times 10^{14}$ s which is obviously impractical. We must therefore consider how far the current experimental techniques need to be extended to provide an interesting result. If the air gap of the etalon were expanded to $g_E = 2$ cm, the counting rate is remarkably increased and the measurement time becomes $t = 9.4 \times 10^6$ s, which corresponds to $t = 110$ days. We believe that such an increase in the air gap, while challenging, is feasible.

A Jamin-type interferometer with large gap etalons is currently under development[35] and further improvements are expected by reducing the etalon dimension to better match the beam path separation requirement and by optimizing the effective lattice constant of multilayers, etc. Details of this work will be published elsewhere.

Kitaguchi et al. reported that they observed a phase drift of unknown origin of ~10 mrad min^{-1}. However, their apparatus was opened to environmental changes in temperature, vibration, magnetic field, and so on. In order to observe the parametric resonance, it will be necessary to isolate the apparatus should or actively canceled these environmental changes as has been done at other facilities [35]. Monitoring or active feedback of the orientation and the gap of etalons using laser interferometers or other techniques could further suppress the phase drift level.

A final concern is the fabrication of the material sample "slabs" with the adjustable gap. The effect of the deviation of the effective potential from the step-like function due to the surface roughness at the level of 0.1 nm remains to be examined.
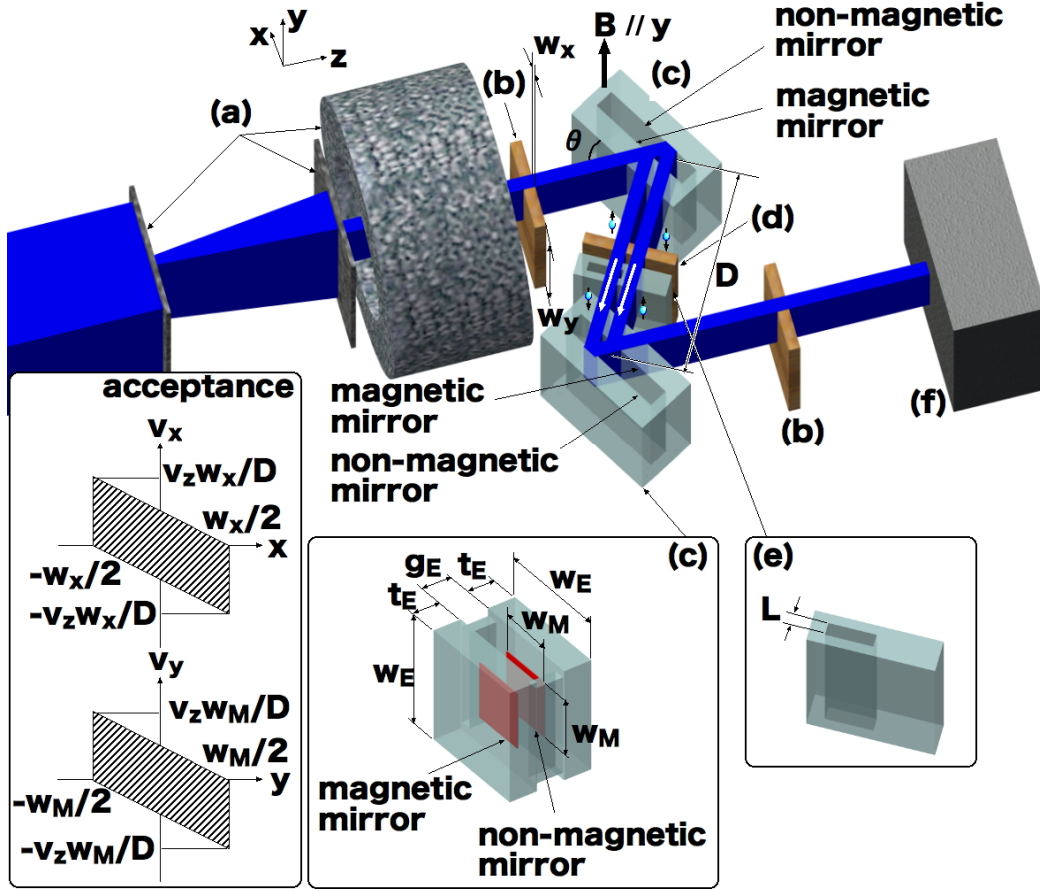
Fig. 6. (Color online) Schematic view of the proposed Kitaguchi-type interferometer. The interferometer comprises of (a) a neutron spin polarizer and neutron beam optics to match the phase space distribution shown in the left inset, (b) a $\pi/2$ flipper, (c) an etalon set with multilayer mirrors deposited on the inner surface of the air-gap, (d) a π flipper, (e) a material plate with a thin gap, (f) a neutron spin analyzer. The left inset shows the acceptance of the interferometer to avoid the beam path overlap between two etalon sets. Central and right insets are enlarged drawing of an etalon set and the material plate, respectively.
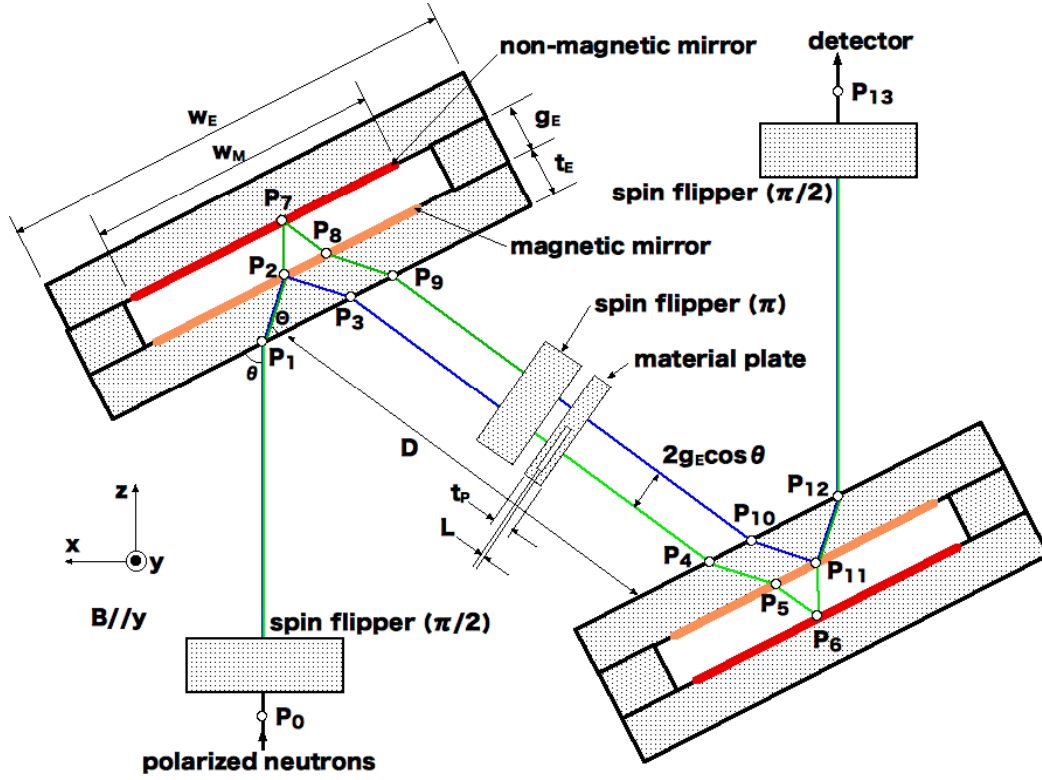
Fig. 7. (Color online) Enlarged top view of the proposed interferometer. Two beam paths of a principal ray are shown in the figure.

Appendix A

For a qualitative understanding of the main features of the solution and a general feature of PR in the transmission amplitude we use a very simple "toy" model related to a solution of only one equation with a characteristic potential which appears in the two-slab interferometer. Then, like in the time-dependent solution of the harmonic oscillator with a solvable Eckart's potential, one can, taking into account the identity,

$$\cosh(x/\lambda) = \frac{\sinh(L/\lambda)}{(L/\lambda)} + \sum_{n=1}^{\infty}\left(\frac{2(-1)^n(L/\lambda)\sinh(L/\lambda)}{(L/\lambda)^2 + n^2\pi^2}\cos\left(\frac{n\pi x}{L}\right)\right), \qquad (8)$$

and rewrite Eq.(2) such that one can represent a factor $k^2(x)$ in the front of the wave

function as a constant (or slowly changing) term plus a periodic

function $k^2(x) = k_{eff}^2[1 + 2\varepsilon\cos(2+\delta)k_{eff}x]$. In this case, according to perturbation

theory, with $|\varepsilon|<<1$ and $|\delta|<<1$, the solution satisfies the parametric resonance

condition. That is, the argument of the cosine is an integral fraction of the double

value of the "frequency": $2k_{eff}/n_0$ with n_0 integral. A quantum parametric resonance

appears for $n_0=1$ when

$$2k_0\bigg/\left(1+\eta\frac{\sinh(L/\lambda)}{(L/\lambda)}\right) = \frac{n\pi}{L}. \qquad (9)$$

For very small η, ($\eta\sinh(L/\lambda)/(L/\lambda)<<1$). This condition is satisfied for

gravitational interactions. This can be simplified as

$$\lambda_n \simeq 4L/n, \qquad (10)$$

where $\lambda_n = 2\pi/k_0$ is neutron wavelength, and is not to be confused with the range of

gravitational interaction λ. It is important to note that while the PR resonance leads

to a very noticeable enhancement, this enhancement occurs only within a very narrow

parameter space. Since the width of the resonance γ (which is defined as a region of

instability for the solution of Schrödinger's equation) decreases with the order of the

harmonic as γ^{n_0}, it is probably only practical to observe resonance effects only for

$n_0=1$.

To understand how the width of the resonance is related to the relevant parameters,

one can use well the known result for the size of the region of instability for a

differential equation with $k^2(x) = k_{eff}^2[1 + 2\varepsilon\cos(2+\delta)k_{eff}x]$ as $\gamma \approx 2\varepsilon k_{eff}$ (see, for

example [36] and [23]). For our case, this gives

$$\gamma / k_{eff} \simeq \frac{a^2 \lambda_n^2}{\pi^2} \frac{(L / \lambda) \sinh(L / \lambda)}{(L / \lambda)^2 + 16\pi^2 (L / \lambda_n)^2} e^{-L/(2\lambda)}. \tag{11}$$

Recall that a^2 is proportional to λ^2, as can be seen from the definition of

$a^2 = 4\pi G \alpha_G m_n^2 \rho \lambda^2 / \hbar^2$. In the same way [23] one can show that the strength of the

resonance is proportional to the characteristic parameter $r \sim (\lambda^2 \alpha_G)^2 \lambda_n^4$.

Therefore, one concludes that, to be able to observe this resonance in practice, one

must work with rather long neutron wavelengths. It should be noted again that the

above formulas are related to the "toy" model and cannot be used for qualitative

analysis of PR in neutron interferometry; for this case we provide numerical solutions

of coupled Schrödinger's equations.

Appendix B

Then, Schrödinger's equation for neutron propagation in between the slabs can be

written as

$$d^2\psi(x) / dx^2 + k^2(x)\psi(x) = 0, \tag{12}$$

where

$$k^2(x) = k_0^2 (1 + \eta \cosh(x / \lambda)),$$

$$\eta = 2a^2 \exp(-L / 2\lambda) / k_0^2,$$

$$a^2 = 4\pi G \alpha_G m_n^2 \rho \lambda^2 / \hbar^2,$$

and k_0 is the neutron wave number in vacuum.

For the left and right "semi-infinite" slabs

$$k^2(x) = k_m^2 (1 + \eta_L \exp(x / \lambda)),$$

and

$$k^2(x) = k_m^2 (1 + \eta_R \exp(-x / \lambda)),$$

where $\eta_L = a^2(1-\exp(-L/\lambda))/k_m^2$, $\eta_R = a^2(\exp(L/\lambda)-1)/k_m^2$, and k_m is the neutron

wave number in material of the slab.

Since we are interested in a special case of η, η_L, $\eta_R \ll 1$, the above equations could

be written in a generic form as

$$d^2\psi(z)/dz^2 + k^2(1+\varepsilon\cosh(z))\psi(z) = 0 \tag{13}$$

and

$$d^2\psi(z)/dz^2 + k^2(1+\varepsilon\exp(z))\psi(z) = 0, \tag{14}$$

assuming that $z = x/\lambda$ and k is an appropriate constant ($k = k_0\lambda$ for Eq.(13) and

$k = k_m\lambda$ for Eq.(14)) with a corresponding ($\varepsilon = \eta$ or $\varepsilon = \eta_R, \eta_L$) small parameter

$\varepsilon \ll 1$.

First let us consider Eq.(13), which is a standard modified Mathieu equation. In our

case, $k^2 > 0$, which leads to oscillating type of solutions, rather than exponentially

decaying solutions usually considering for a modified Mathieu equation (where k^2 is

assumed to be a negative constant). For the case of $\varepsilon = 0$ the solution describes free

particle propagation

$$\psi_0(z) = a\exp(\pm ikz) = a\exp(\pm i\varphi(z)) \tag{15}$$

with a phase $\varphi(z) = kz = k_0 x$.

If $\varepsilon > 0$, using Liouville's transformation one can see[37] that Eq.(13) has a pair of

solutions with the following asymptotics as $z \to \infty$:

$$(\varepsilon k^2 \cosh(z))^{-1/4} \exp\left(\pm ik\int_{z_0}^{z}\sqrt{1+\varepsilon\cosh(z)}dz\right)(1+o(1)). \tag{16}$$

Therefore, the phase becomes

$$\varphi(z) \to kz + k\sinh(z)\varepsilon/2, \tag{17}$$

which leads to exponential enhancement of the contribution to the phase from the

small parameter ε on the neutron propagation path L

$$\varphi(L) \approx k_0 L + \varepsilon(k_0\lambda)\exp(L/\lambda)/2. \tag{18}$$

The same enhancement of the phase of the transmission coefficient can be obtained

for a specific set of parameters $\lambda_n = \pi\lambda$ of the Eq.(2), which transform it to a

"standard" form of modified Mathieu equation

$$d^2\psi(x)/dx^2 + k_0{}^2(1+\eta\cosh(2k_0x))\psi(x) = 0.$$ (19)

By changing variables $z = \exp(k_0x)$ and assuming $\psi(z) = y(z)/\sqrt{z}$, the above

equation transforms into

$$\frac{d^2y(z)}{dz^2} + \left(\frac{\eta}{2z^4} + \frac{5}{4z^2} + \frac{\eta}{2}\right)y(z) = 0.$$ (20)

Thus, for large z, the asymptotic solution is $y(z) \sim \exp(\pm i\sqrt{\eta/2}z)$ which leads to the

asymptotic phase for a solution of Eq.(19)

$$\psi(x) \sim \exp\left(\pm ik_0\sqrt{\frac{\eta}{2}}\exp(k_0x)\right)$$ (21)

instead of the "expected" plane wave asymptotic $\exp(\pm ik_0x)$. Thus, one can see that

in the region of possible instability (PR), the phase related to the small interaction (η)

is increasing exponentially (a characteristic behavior of PR), while the "regular"

interaction leads to linear phase $\exp(\pm ik_0x)$. It should be noted that more careful

derivation (see, for example [38],[39]) of the asymptotic solution of Eq.(19) leads to the

phase

$$\psi(x) \sim \exp\left(ik_0\sqrt{\frac{\eta}{2}}sinh(k_0x)\right).$$

One can obtain an asymptotic solution for Eq.(13) by transforming it with

$\psi(z) = \exp\left\{k\int^z w(z)dz\right\}$, where $w(z)$ is a differentiable function of z (see, for example

[43]). Then, since

$$\frac{d\psi}{dz} = kw\psi, \qquad \frac{d^2\psi}{dz^2} = k\psi\left(\frac{dw}{dz} + kw^2\right)$$

one obtains a Riccati equation

$$\frac{1}{k}\frac{dw}{dz} + w^2 + \rho^2 = 0 \tag{22}$$

where $\rho^2 = (1 + \varepsilon \cosh(z))$ which gives for $k \gg 1$

$$\psi(z) \sim \exp\left(\pm ikz \mp ik(\varepsilon/4)\sinh z\right) \tag{23}$$

This is a different asymptotic regime but the exponentially growing phase is presented

here as well. It should be noted that the presence of exponentially enhanced terms

related to a small parameter ε in the solution of Eq.(13) is clearly seen from a

representation of the solution in terms of Bessel functions in the Appendix 1 of the

book [40] (see also [40] for calculation of Bessel functions for imaginary order). All

these results are in agreement with detailed investigation of uniform asymptotic form

of modified Mathieu functions in a complex domain [41].

Now, one can obtain an equation for a phase of the solution of Eq.(13) using the Van

der Pol variables (see, for example [42]) for amplitude z and phase φ provided

$$\psi = z\cos\varphi$$
$$\psi' = -kz\sin\varphi \tag{24}$$

Then the phase satisfies the non-linear equation

$$\varphi'(z) = k + \varepsilon \cosh z \cos^2 \varphi(z) \tag{25}$$

which, with the considered above the existence of exponentially growing phase,

indicates the possibility of unstable solutions. To show the existence of the

exponentially grooving solution on can use perturbation theory expansion as

$\varphi = \varphi_0 + \varepsilon\varphi_1 + \varepsilon^2\varphi_2...$ where $\varphi_0 = kz$. And each term $\varphi_m \sim (\cosh z)^m$. For the case of

extremely slow neutrons $(k \to 0)$ this sum results in $\varphi = kz + \tan^{-1}(\varepsilon \cdot \cosh z)$ where

$\varepsilon \sim \lambda_n^2$.

One can observe that Eqs. (13) and (14) can be transformed into double-confluent

Heun (DCHE) equation (see, for example [43],[44],[45]), which is a subject of recent

intensive studies due to important applications to gravitation and cosmology. The

DCHE could be written [46] as

$$\frac{d^2 y(z)}{dz^2} + \left(A + \frac{B}{z} + \frac{C}{z^2} + \frac{D}{z^3} + \frac{E}{z^4} \right) y(z) = 0$$

with a set of parameters A, B, C, D, and E. One can see that it exactly match Eq.(20).

Therefore, one can conclude that the enhancement of a phase which was discussed for exponential and hyperbolic cosine potential is a generic feature for the inverse forth-power potential. In other words, one can expect that phase of the solution of Heun equation in vicinity of irregular points can be unstable, i.e. to lead to a parametric phase enhancement. This is exactly confirmed by the set of known applications of the Heun equations for the one-dimensional Schrodinger equation for exactly solvable potentials (see, i.e., [46], [47] and references therein). For example, for the potential [48] of Cho and Ho

$$V(x) = -\frac{b^2}{4} e^{2x} - (l+1) d e^{-x} + \frac{d^2}{4} e^{-2x} \tag{26}$$

the wave function [48] has an explicit phase factor $\sim \exp(i b e^x / 2)$. More examples for exponentially grooving potentials are to be found in [48]. The study of the inversed power potential $\sim \lambda (x_0/x)^n$ leads to a singular phase [49] in the vicinity of $x=0$

$$\sim \frac{2}{n-2} \left(\lambda \left(\frac{x_0}{x} \right)^{n-2} \right)^{1/2}$$

For a detailed analysis for $\sim 1/x^4$ potential see [50].

It is worth to note that using [51] the expression

$$\cosh(x/\lambda) = \frac{\sinh(L/\lambda)}{(L/\lambda)} + \sum_{n=1}^{\infty} \left(\frac{2(-1)^n (L/\lambda) \sinh(L/\lambda)}{(L/\lambda)^2 + n^2 \pi^2} \cos \left(\frac{n \pi x}{L} \right) \right), \tag{27}$$

Eq.(13) can be re-written as a Hill's equation for a specific value of L:

$$\frac{d^2 y(z)}{dz^2} + \left(a + \sum_{n=1}^{\infty} a_n \cos(2nz) \right) y(z) = 0$$

which usually describes parametric excitations of complex systems.

We conclude that one dimensional Schrodinger equation with exponential, hyperbolic and inversed power potentials belong to the class of Heun differential equations which have a regions of unstable (exponentially grooving) solutions. For a number of particular cases we observed that a phase of the solution of the Schrodinger equation has exponentially grooving part which could lead to an unstable solution, or a phase parametric resonance which was found numerically in [17] for the transmission coefficient for neutron propagation.

[1] E. G. Adelberger, B. R. Heckel, and A. E. Nelson, Annu. Rev. Nucl. Part. Sci. **53**, 77 (2003).

[2] N. Arkani-Hamed, S. Dimopoulos, and G. Dvali, Phys. Lett., B **429**, 263 (1998).

[3] I. Antoniadis, N. Arkani-Hamed, S. Dimopoulos, and G. Dvali, Phys. Lett., B **436**, 257 (1998).

[4] L. Randall and R. Sundrum, Phys. Rev. Lett. **83**, 4690 (1999).

[5] V. A. Rubakov, Phys. Usp. **44**, 871 (2003).

[6] R. Sundrum, Phys. Rev. D **69**, 044014 (2004).

[7] A. Zee, Phys. Lett. B **594**, 8 (2004).

[8] Review of Particle Physics, J. Phys. G **33**, 225 (2006).

[9] D. N. Spergel *et al*., ApJS **170**, 377 (2007).

[10] H. Goldberg and P. Nath, arXiv:0706.3898 (2007).

[11] H. Georgi, Phys. Rev. Lett. **98**, 221601 (2007).

[12] H. Leeb and J. Schmiedmayer, Phys. Rev. Lett. **68**, 1472 (1992).

[13] V. V. Nesvizhevsky and K. V. Protasov, Class. Quant. Grav. **21**, 4557 (2004); V. V. Nesvizhevsky and K. V. Protasov, J. Res. Natl. Inst. Stand. Technol. **110**, 269 (2005).

[14] O. Zimmer and N. Kaiser, arXiv:hep-ph/0602127 (2006).

[15] V. V. Nesvizhevsky, G. Pignol, and K. V. Protasov, Phys. Rev **D 77**, 034020 (2008).

[16] R. R. Caldwell and D. Grin, arXiv: astro-ph/0606133 (2006).

[17] G. L. Greene and V. Gudkov, Phys. Rev. C **75**, 015501 (2007).

[18] H. Kogelnik and T. Li, Appl. Opt. **5**, 1550 (1966).

[19] A. E. Seigman, *Lasers* (University Science, Mill Valley, CA, 1986)

[20] A. Hardy, Appl. Phys. **18**, 223 (1979).

[21] S. Longhi, Opt. Comm. **176**, 327 (2000).

[22] E. Kh. Akhmedov, Nucl. Phys. B **538**, 25 (1999); E. Kh. Akhmedov, Phys. Atom. Nucl. **64**, 781 (2001).

[23] A. M. Perelomov and Ya. B. Zel'dovich, *Quantum Mechanics - Selected Topics* (World Scientific Publishing Co. Pte. Ltd., Singapore, New York, London, 1998)

[24] C. Eckart, Phys. Rev. **35**, 1303 (1930).

[25] M. S. Marinov and Bilha Segev, J. Phys. A: Math. Gen. **29**, 2839 (1996).

[26] L. D. Faddeev, Trudy Mat. Inst. Steklov **73**, 314 (1964); L. D. Faddeev, Am. Math Soc. Transl. **2**, 139 (1967).

[27] R. G. Newton, J. Math Phys. **21**, 493 (1980).

[28] M. Sassoli de Bianchi, J. Math. Phys. **35**, 2719 (1994); M. G. Rozman, P. Reineker, and R. Tehver, Phys. Rev. A **49**, 3310 (1994); Y. Nogami and C. K. Ross,

Am. J. Phys. **64**, 923 (1996); K. A. Kiers and W. van Dijk, J. Math. Phys. **37**, 6033 (1996).

29 P. M. Morse and H. M. Feshbach, *Methods of Theoretical Physics* (Feshbach Publishing, LLC, Minneapolis, 1981), Vol. **2**.

30 L. D. Landau and E. M. Lifshitz, *Quantum Mechanics*, **3**rd edition (Butterworth-Heinemann, Oxford, 2002), Vol. **3.**

31 H. Rauch and S. Werner, *Neutron Interferometry* (Oxford University Press, USA , 2000).

32 M. Kitaguchi *et al*., Phys. Rev. A **67**, 033609 (2003).

33 ILL Instrument Description http://www.ill.fr/YellowBook/PF2

34 A. Steyerl *et al*., Phys. Lett. A **116**, 347 (1986).

35 K Yamamura, Annals of CIRP **56**, 541 (2007).

36 L. D. Landau and E. M. Lifshitz, *Mechanics*, **3**rd edition (Butterworth-Heinemann, Oxford, 2002), Vol. 1**.**

37 F. A. Berezin and M. A. Shubin, *The Schrodinger Equation* (Kluwer Academic Publishers, Netherlands, 1991).

38 E. T. Whittaker and G. N. Watson, *A course of modern analysis* (Cambridge University Press, Cambridge, UK, 2005).

39 N. W. McLachlan, *Theory and application of Mathieu functions* (Dover Publications, Inc., New York, 1964)

40 A. Gil, J. Segura, and N. M. Temme, ACM Tran. on Math. Software **2**, 145 (2004).

41 A. Sharples, Quart. J. Mech. and Applied Math. **20**, 365 (1967).

42 N. N. Moiseev, *Asymptotic methods of non-linear mechanics* (Nauka, Moscow, 1981)

[43] F. M. Arscott, *Periodic Differential Equations* (Permagon Press, New York, 1964)

[44] S. Yu. Slavyanov and W. Lay, *Special Functions. A Unified Theory Based on Singularities* (Oxford University Press, New York, 2000).

[45] A. Ronveaux, *Heun's differential Equetions* (Oxford University Press, New York, 1995).

[46] Lea Jaccoud El-Jaick and Bartolomeu D. B. Figueiredo, arXiv:0807.2219.

[47] Lea Jaccoud El-Jaick, Bartolomeu D. B. Figueiredo, preprint CBPF-NF-003/08.

[48] H. T. Cho and C. L. Ho, J. Phys. A **40**, 1325 (2007).

[49] K. M. Case, Phys. Rev. **80**, 797 (1950).

[50] H. J. M. Muller-Kirsten, *Introduction to Quantum Mechanics. Schrodinger equation and Path Integral* (World Scientific Publishing, Singapore, 2006).

[51] V. Gudkov, H. M. Shimizu, and G. L. Greene, NIM **A611**, 153 (2009).